

Impaired dopamine release and synaptic plasticity in the striatum of *Parkin*^{-/-} mice

Tohru Kitada,* Antonio Pisani,†‡ Maha Karouani,§ Marian Haburcak,§ Giuseppina Martella,†‡ Anne Tscherter,†‡ Paola Platania,†‡ Bei Wu,* Emmanuel N. Pothos§ and Jie Shen*

*Program in Neuroscience, Center for Neurologic Diseases, Brigham & Women's Hospital, Harvard Medical School, Boston, Massachusetts, USA

†Department of Neuroscience, University of Rome Tor Vergata, Rome, Italy

‡Fondazione Santa Lucia IRCCS, Rome, Italy

§Department of Pharmacology and Experimental Therapeutics and Program in Neuroscience, Tufts University School of Medicine, Boston, Massachusetts, USA

Abstract

Parkin is the most common causative gene of juvenile and early-onset familial Parkinson's diseases and is thought to function as an E3 ubiquitin ligase in the ubiquitin-proteasome system. However, it remains unclear how loss of Parkin protein causes dopaminergic dysfunction and nigral neurodegeneration. To investigate the pathogenic mechanism underlying these mutations, we used *parkin*^{-/-} mice to study its physiological function in the nigrostriatal circuit. Amperometric recordings showed decreases in evoked dopamine release in acute striatal slices of *parkin*^{-/-} mice and reductions in the total catecholamine release and quantal size in dissociated chromaffin cells derived from *parkin*^{-/-} mice. Intracellular recordings of striatal medium spiny neurons

revealed impairments of long-term depression and long-term potentiation in *parkin*^{-/-} mice, whereas long-term potentiation was normal in the Schaeffer collateral pathway of the hippocampus. Levels of dopamine receptors and dopamine transporters were normal in the *parkin*^{-/-} striatum. These results indicate that Parkin is involved in the regulation of evoked dopamine release and striatal synaptic plasticity in the nigrostriatal pathway, and suggest that impairment in evoked dopamine release may represent a common pathophysiological change in recessive parkinsonism.

Keywords: dopamine transporter, dopaminergic, knockout, mouse.

J. Neurochem. (2009) **110**, 613–621.

Parkinson's disease (PD) is a common, progressive neurodegenerative disorder that is clinically characterized by resting tremor, bradykinesia, rigidity, and postural imbalance. It is neuropathologically characterized by the loss of nigral neurons, resulting in impaired dopaminergic projection to the striatum. Since the identification of the causative mutations in the *parkin* gene for autosomal recessive juvenile parkinsonism (AR-JP) in 1998, a large variety of mutations have been found among different ethnic groups throughout the world (Hattori *et al.* 1998; Kitada *et al.* 1998; Lucking *et al.* 2000; Hedrich *et al.* 2004). Because Parkin functions as an E3 ubiquitin ligase in the ubiquitin proteasome system, loss of Parkin function is thought to cause an accumulation of excess target proteins through failure in their degradation (Shimura *et al.* 2000).

The disease usually has a very early onset before the age of 40 and has some specific clinical features of prominent

sleep benefit/diurnal fluctuation, morning foot dystonia, a tendency to develop dyskinesias in response to levodopa, and psychiatric problems in addition to typical parkinsonian tetrads (Yamamura *et al.* 1973, 2000). Although these symptoms suggest the presence of abnormal dopaminergic metabolism or signaling in the patients, the underlying

Received March 24, 2009; revised manuscript received April 25, 2009; accepted April 30, 2009.

Address correspondence and reprint requests to Jie Shen, Program in Neuroscience, Center for Neurologic Diseases, Brigham & Women's Hospital, Harvard Medical School, Boston, MA 02115, USA.
E-mail: jshen@rics.bwh.harvard.edu

Abbreviations used: AR-JP, autosomal recessive juvenile parkinsonism; DA, dopamine; DAT, dopamine transporter; EPSP, excitatory postsynaptic potential; HFS, high-frequency stimulation; LTD, long-term depression; LTP, long-term potentiation; MSN, medium spiny neurons; PD, Parkinson's disease; TBS, theta burst stimulation.

pathophysiological mechanism is unknown. Moreover, some PD patients carry various single heterozygous *parkin* mutations, suggesting low penetrance associated with reduced *parkin* dosages (Foroud *et al.* 2003; Sun *et al.* 2006).

Recent clinical studies for other recessive PD genes, i.e., *DJ-1* and *PINK1*, showed that in addition to typical parkinsonian features, patients carrying mutations in *DJ-1* or *PINK1* sometimes also exhibit specific clinical features that are similar to those of patients carrying *parkin* mutations (Bonifati *et al.* 2002; Dekker *et al.* 2003; Albanese *et al.* 2005). These findings suggest that loss of function mutations in these three genes may cause similar dopaminergic impairment. In fact, *DJ-1* and *PINK1* knockout mice exhibit reduced dopamine (DA) overflow and impaired striatal synaptic plasticity (Goldberg *et al.* 2005; Kitada *et al.* 2007). These results imply that *parkin* insufficiency may cause a similar impairment in the dopaminergic circuit.

To investigate the pathogenic mechanisms underlying *parkin* mutations, we performed functional analysis of the nigrostriatal circuit in *parkin* knockout mice. Amperometric recordings revealed decreases in evoked DA release in acute striatal slices of *parkin*^{-/-} mice. Consistent with this result, total catecholamine release and quantal size are also reduced in dissociated chromaffin cells derived from homozygous and heterozygous *parkin* knockout mice. Furthermore, intracellular recordings of striatal medium spiny neurons (MSNs) revealed specific impairments of long-term depression (LTD) and long-term potentiation (LTP) in *parkin* knockout mice, whereas hippocampal LTP is normal.

Materials and methods

Mice

Parkin^{-/-} mice bearing a germline disruption of exon 3 and wild-type controls were obtained from *parkin*^{+/-} mice intercross in the hybrid background of C57BL/6 and 129/Sv as previously described (Goldberg *et al.* 2003). Mice used for amperometric recordings were female at the age of 8–16 weeks. Mice used for intracellular recordings were gender-balanced at the age of 8–11 weeks.

Amperometric recording

Acute coronal striatal slices and carbon fiber microelectrodes (7 μ m tip diameter) were prepared as described elsewhere (Kitada *et al.* 2007). A constant monophasic current stimulus was applied to the site of recording through a bipolar stimulating electrode. Parameters of stimulation included single rectangular pulse of 2 ms, +500 μ A amplitude; a train of five single pulses was delivered with an interstimulus interval of 5 min to allow full recovery. Local bath application of the DA reuptake blocker, nomifensine (3 μ M), for at least 30 min was also used in order to assess the contribution of reuptake in the evoked DA signal. Data acquisition occurred at 50 kHz and was digitally post-filtered at 1 kHz. Data analysis included spike amplitude, spike width, and number of molecules as derived by the charge of each spike. Estimates were based on an assumption of two electrons donated per oxidized molecule of DA

(Ciolkowski *et al.* 1994). Amperometric spikes were identified as events with greater than 4.5 \times the root mean square noise of the baseline following the stimulus artifact. The five single pulses per slice were averaged into a grand mean and the means of the values obtained from the two genotypic groups were compared with One-way ANOVA.

For preparation of primary dissociated adrenal chromaffin cells, dissected medullae were minced into pieces and dissociated by incubation at 37°C with Ca²⁺-free collagenase subtype IA solution (0.2%) for 35 min. The digested tissues were triturated gently in 1% bovine serum albumin and 0.02% deoxyribonuclease. The dissociated cells were resuspended in a medium composed of Dulbecco's modified Eagle's medium, 10% fetal bovine serum, 50 U/mL penicillin, and 50 μ g/mL streptomycin. The cell suspension was placed onto laminin-coated glass wells in 35-mm dishes, and flooded with Dulbecco's modified Eagle's medium-based culture medium. Cells were maintained in a 5% CO₂ incubator at 37°C. Amperometric recordings were taken between days 1 and 3 post-plating with carbon fiber microelectrodes (5 μ m tip diameter). Amperometric recordings were monitored from individual chromaffin cells after picospritzing an 80 mM K⁺ solution for 6 s on each cell. Data acquisition occurred at 50 kHz and was digitally post-filtered at 1 kHz. Statistical significance was analysed through One-way ANOVA of the means for quantal size, amplitude, width, and interspike interval.

Intracellular recordings for MSNs

Cortico-striatal slices (180–250 μ m) were prepared as previously described (Kitada *et al.* 2007). Coronal slices were cut in Krebs' solution (in mM: 126 NaCl, 2.5 KCl, 1.3 MgCl₂, 1.2 NaH₂PO₄, 2.4 CaCl₂, 10 glucose, and 18 NaHCO₃), bubbled with 95% O₂ and 5% CO₂. Individual slices were transferred in a recording chamber (~1 mL volume), continuously superfused with oxygenated Krebs' medium, at 2.5–3 mL/min (32–33°C). Current clamp recordings were performed from MSNs using sharp microelectrodes filled with 2 M KCl (40–60 M Ω). Signal acquisition and off-line analysis was performed using an Axoclamp 2B amplifier and pClamp9 software (Axon Instruments, Foster City, CA, USA). Cortico-striatal excitatory post-synaptic potentials (EPSPs) were evoked with a bipolar electrode placed in the corpus callosum. Test stimuli were delivered at 0.1 Hz in 10 μ M bicuculline to avoid contamination with GABA-A currents. For high-frequency stimulation (HFS, three trains: 3 s duration, 100 Hz frequency, 20 s intervals), stimulus intensity was raised to suprathreshold levels. For each recorded cell, the EPSP amplitude was averaged every 20 s. This value was plotted as a percentage of the averaged EPSP amplitude during a stable period of at least 15 min preceding HFS. Values given were mean \pm SEM. Student's *t*-test and ANOVA test were used to assess statistical significance. *Post hoc* Tukey test was performed among groups (α = 0.01). Amphetamine was a generous gift of Nicola B. Mercuri. SKF and quinpirole were obtained from Tocris Cookson (Bristol, UK), bicuculline was obtained from Sigma (Milan, Italy).

Hippocampal electrophysiology

Acute hippocampal slices (400 μ m) were cut and maintained in artificial cerebrospinal fluid (in mM: 119 NaCl, 2.5 KCl, 1 NaH₂PO₄, 2 MgCl₂, 2 CaCl₂, 26 NaHCO₃, and 11 dextrose, pH 7.4) at 30°C as described (Saura *et al.* 2004). Stimulation (200 μ s) pulses were delivered with a bipolar concentric metal electrode. Synaptic strength was quantified as the initial slope of field potentials

recorded with artificial CSF-filled microelectrodes (~1 MΩ). Baseline responses were collected every 15 s with a stimulation intensity that yielded 50–60% of maximal response. LTP was induced by five episodes of theta burst stimulation (TBS) delivered at 0.1 Hz. Each episode contained 10 stimulus trains (four pulses at 100 Hz) delivered at 5 Hz. Average responses (mean ± SEM) were expressed as percent of pre-TBS baseline response. Repeated measures ANOVA and non-paired *t*-test were used to assess statistical significance.

Radioligand binding autoradiography

Ligand labeling for D₁-like and D₂-like receptor sites was essentially carried out as described in (Kitada *et al.* 2007). Briefly, to measure the density of D₁-like receptor sites, slide-mounted brain sections (20 μm) were incubated for 1 h at 25°C in 50 mM Tris-HCl (pH 7.4) containing 4 mM MgCl₂ and 1 nM [³H]-SCH23390 (85.0 Ci/mmol; PerkinElmer, Waltham, MA, USA). Non-specific binding was determined using 1 μM unlabeled SCH23390 (Sigma). To measure D₂-like receptor sites, brain sections were incubated for 1 h at 25°C in specific incubation buffer containing 0.6 nM [³H]-spiperone (15.0 Ci/mmol; PerkinElmer). Non-specific binding was defined using 10 μM unlabeled spiperone (Sigma). After incubation, brain sections were rinsed twice in the respective incubation buffer for 5 min each time. After air dry, sections were placed on imaging plates (BAS-TR2025; Fujifilm, Stamford, CT, USA). The imaging plates were scanned with a high-performance imaging plate reader (BAS5000; Fuji film). Quantitative analysis of the radioactivity was processed by the image analysis software (Multi Gauge V3.0; Fuji film). Seven to ten serial coronal sections every 100 μm were used for each animal to calculate the mean radioactivity of the striatum.

[³H]DA reuptake assay

The striata were dissected out and homogenized in 20 volumes of ice-cold 0.32 M sucrose using a Teflon homogenizer. Homogenates were centrifuged at 1000 *g* for 10 min at 4°C. Supernatants were removed and centrifuged at 17 500 *g* for 30 min at 4°C. The pellets of crude synaptosomes were resuspended in ice-cold modified Krebs's assay buffer (in mM: 126 NaCl, 4.8 KCl, 1.25 CaCl₂, 1.4 MgSO₄, 16.4 NaH₂PO₄, 11 glucose, 1.14 ascorbate, 1 pargyline, 5 desipramine, and 1 fluoxetine, pH 7.4). One mL assay buffer in each tube contained 62.5 nM [³H]DA (PerkinElmer). After pre-incubation of the assay tubes for 10 min at 37°C, assays were initiated by addition of 80 μL synaptosomal tissue homogenate containing about 20 μg protein. Samples were incubated at 37°C for 6 min. Then, the reaction was terminated by adding 3 mL of cold assay buffer and rapid filtration through Whatman GF/B filters (Whatman Inc., Piscataway, NJ, USA) soaked previously in 0.05% polyethylenimine. Non-specific uptake was determined in the presence of 1 mM DA hydrochloride (Sigma) and 62.5 nM [³H] DA. Radioactivity trapped in filters was counted using a liquid scintillation counter (Beckman Coulter Inc., Fullerton, CA, USA).

Results

Reduction of evoked DA release in *parkin*^{-/-} striatal slices

To examine the function of Parkin in the dopaminergic system, we performed amperometric recordings using acute

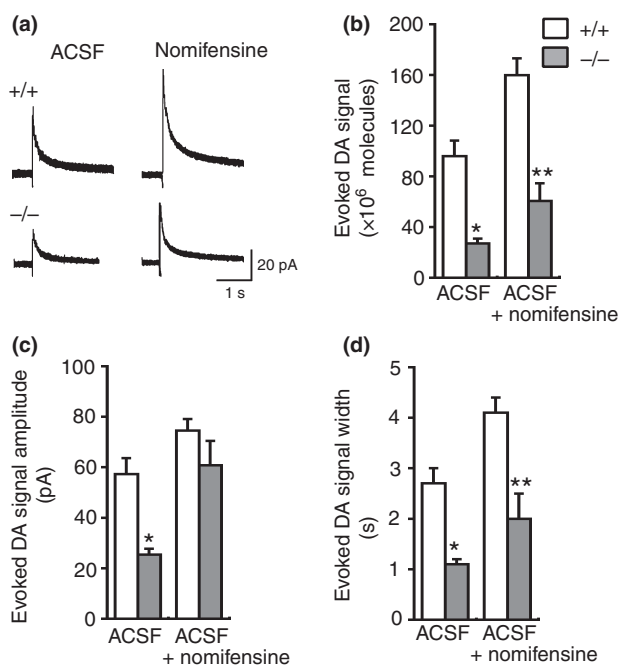


Fig. 1 Reduced evoked DA release in acute striatal slices of *parkin* knockout mice. (a) Decreased evoked DA release in the dorsal-dorsomedial striatum of *parkin*^{-/-} mice. Representative amperometric traces of electrical stimulation-evoked DA release are presented on the left. (b) Mean evoked DA signal from *parkin*^{-/-} slices was lower than *parkin*^{+/+} slices (+/+ : 96.0 ± 12.1 × 10⁶ molecules; -/- : 27.0 ± 3.8 × 10⁶ molecules, **p* < 0.05). After 30 min exposure to nomifensine, the number of molecules from *parkin*^{+/+} slices was 155.9 × 10⁶ ± 13.1 × 10⁶ whereas the molecule number from *parkin*^{-/-} slices was again lower at 60.6 × 10⁶ ± 14.0 × 10⁶ (***p* < 0.01). (c) Mean evoked DA signal amplitude from *parkin*^{-/-} slices was significantly lower (+/+ : 57.3 ± 6.3 pA; -/- : 25.4 ± 2.3 pA, **p* < 0.05). However, mean spike amplitude from *parkin*^{-/-} slices in nomifensine was unchanged (+/+ : 74.5 ± 4.6 pA; -/- : 60.8 ± 9.6 pA, *p* > 0.05). (d) Similarly, slices from *parkin*^{-/-} mice showed a lower mean evoked DA signal width (+/+ : 2.7 ± 0.3 s; -/- : 1.1 ± 0.1 s, **p* < 0.05). After nomifensine, the mean width from *parkin*^{-/-} slices was also much lower (+/+ : 4.1 ± 0.3 s; -/- : 2.0 ± 0.5 s, ***p* < 0.01). Data are presented as mean ± SEM. aCSF, artificial cerebrospinal fluid.

dorsal striatal slices from *parkin*^{-/-} mice and wild-type controls (Fig. 1a). Mean evoked DA signal in *parkin*^{-/-} mice was significantly lower than in *parkin*^{+/+} mice (+/+ : 96.0 ± 12.1 × 10⁶ molecules, *n* = 50 events from 10 slices; -/- : 27.0 ± 3.8 × 10⁶ molecules, *n* = 35 events from seven slices, *p* < 0.05 by One-way ANOVA; Fig. 1b). Mean evoked DA signal amplitude in *parkin*^{-/-} mice was also significantly lower (+/+ : 57.3 ± 6.3 pA; -/- : 25.4 ± 2.3 pA, *p* < 0.05; Fig. 1c). Similarly, slices from *parkin*^{-/-} mice showed lower mean evoked DA signal width (+/+ : 2.7 ± 0.3 s; -/- : 1.1 ± 0.1 s, *p* < 0.05; Fig. 1d). These results demonstrated that *parkin* inactivation caused a marked decrease in evoked DA signal.

Next, to determine whether the DA decrease was caused by an impaired DA release from vesicles or changes in DA reuptake by DA transporters (DAT), we performed amperometric recordings in the presence of the DA reuptake blocker, nomifensine (3 μ M). In the presence of nomifensine, mean evoked DA signal in *parkin*^{-/-} mice remained lower than in *parkin*^{+/+} mice (+/+ : $155.9 \pm 13.1 \times 10^6$ molecules, $n = 45$ events from nine slices; -/- : $60.6 \pm 14.0 \times 10^6$ molecules, $n = 35$ events from 7 slices, $p < 0.01$; Fig. 1a and 1b). The mean evoked DA signal width was lower in *parkin*^{-/-} mice (+/+ : 4.1 ± 0.3 s; -/- : 2.0 ± 0.5 s, $p < 0.01$; Fig. 1d). These results indicated that evoked DA release was decreased in the absence of Parkin.

Reduction of evoked catecholamine release in *parkin*^{-/-} and *parkin*^{+/-} chromaffin cells

To investigate further the effects of *parkin* inactivation on catecholamine release, we also performed amperometric recordings on primary dissociated adrenal chromaffin cells, which are thought to share a similar exocytosis mechanism as nigral neurons and permit measurement of monoquantal release in real time from single vesicles (Fig. 2a). In this experiment, we also included analysis of chromaffin cells derived from *parkin*^{+/-} mice, as various single heterozygous *parkin* mutations have been associated with parkinsonism. Total catecholamine release per cell during the 6-sec stimulation was much lower in *parkin*^{-/-} and *parkin*^{+/-} cells than in *parkin*^{+/+} cells (+/+ : $101.5 \pm 12.2 \times 10^6$ molecules, $n = 32$ cells; +/- : $59.0 \pm 12.9 \times 10^6$ molecules, $n = 25$ cells, $p < 0.05$ by *t*-test; -/- : $43.6 \pm 9.9 \times 10^6$ molecules, $n = 24$ cells, $p < 0.01$; Fig. 2b). The mean catecholamine quantal size was also significantly lower in *parkin*^{-/-} and *parkin*^{+/-} cells, but there was no significant difference between *parkin*^{+/-} and *parkin*^{-/-} mice (+/+ : $92.7 \pm 5.2 \times 10^4$ molecules, 3410 vesicles from 32 cells; +/- : $64.4 \pm 8.1 \times 10^4$ molecules, 2502 vesicles from 25 cells, $p < 0.01$; -/- : $54.4 \pm 8.1 \times 10^4$ molecules, 2037 vesicles from 24 cells, $p < 0.01$; Fig. 2c). These results provided further support for a deficit in catecholamine release in *parkin*^{-/-} mice.

Impaired bidirectional synaptic plasticity in *parkin*^{-/-} mice

Similar to the previous report (Goldberg *et al.* 2003), the analysis of the intrinsic membrane properties did not reveal significant changes between *parkin*^{+/+} and *parkin*^{-/-} mice (Martella *et al.* 2009). MSNs from both *parkin*^{+/+} and *parkin*^{-/-} mice (+/+ : $n = 49$; -/- : $n = 66$) were silent at rest, and upon depolarizing current pulses showed membrane rectification and tonic action potential discharge. The current-voltage relationship did not show any relevant changes among groups (data not shown). Mean EPSP amplitude or duration were comparable between *parkin*^{+/+} and *parkin*^{-/-} mice and were fully suppressed by the α -amino-3-hydroxy-5-methylisoxazole-4-propionate receptor

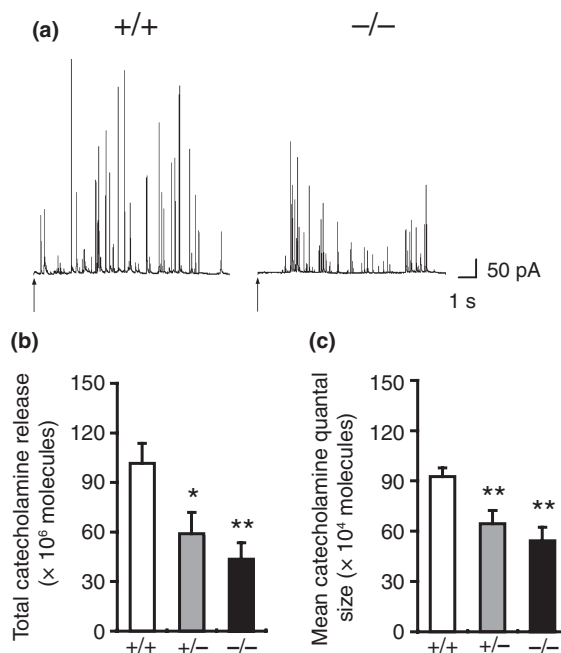


Fig. 2 Reduced evoked catecholamine release in primary dissociated adrenal chromaffin cell cultures from *parkin* knockout mice. (a) Decreased evoked catecholamine release in primary dissociated adrenal chromaffin cells from *parkin*^{-/-} mice. Amperometric traces of 80 mM K⁺-evoked catecholamine release are indicated at the top. Arrows show the onset of high K⁺ stimulation. (b) The mean total catecholamine release was much lower in *parkin*^{-/-} and *parkin*^{+/-} cells (+/+ : $101.5 \pm 12.2 \times 10^6$ molecules; +/- : $59.0 \pm 12.9 \times 10^6$ molecules, * $p < 0.05$; -/- : $43.6 \pm 9.9 \times 10^6$ molecules, ** $p < 0.01$). (c) The mean catecholamine quantal size was also significantly lower in *parkin*^{-/-} and *parkin*^{+/-} cells (+/+ : $92.7 \pm 5.2 \times 10^4$ molecules; +/- : $64.4 \pm 8.1 \times 10^4$ molecules, ** $p < 0.01$; -/- : $54.4 \pm 8.1 \times 10^4$ molecules, ** $p < 0.01$).

antagonist, CNQX (10 μ M) (data not shown, $p > 0.05$). DA exerts a central role in the regulation of corticostriatal synaptic plasticity (Calabresi *et al.* 2007). As expected, HFS in the presence of magnesium induced LTD in MSNs from *parkin*^{+/+} mice ($62.5 \pm 9\%$ of control, measured 20 min post-HFS, $n = 25$, $p < 0.01$; Fig. 3a). Conversely, in MSNs recorded from *parkin*^{-/-} mice, HFS failed to induce LTD ($95.5 \pm 11\%$ of control, $n = 39$, $p > 0.05$; Fig. 3a).

To determine whether the impairment of LTD was caused by defective D₁ receptors, slices were treated with the D₁ receptor agonist SKF38393. In the presence of SKF38393 (10 μ M), however, HFS failed to restore LTD ($92.5 \pm 7\%$, $n = 11$, $p > 0.05$; Fig. 3b). Likewise, bath application of the D₂-like receptor agonist quinpirole (10 μ M) was unable to restore LTD in *parkin*^{-/-} mice ($86.4 \pm 17\%$, $n = 11$, $p > 0.05$; Fig. 3b). Because LTD induction has been shown to require co-activation of both D₁ and D₂ of DA receptors (Calabresi *et al.* 2007), we treated slices with both SKF38393 and quinpirole. Under these conditions, HFS

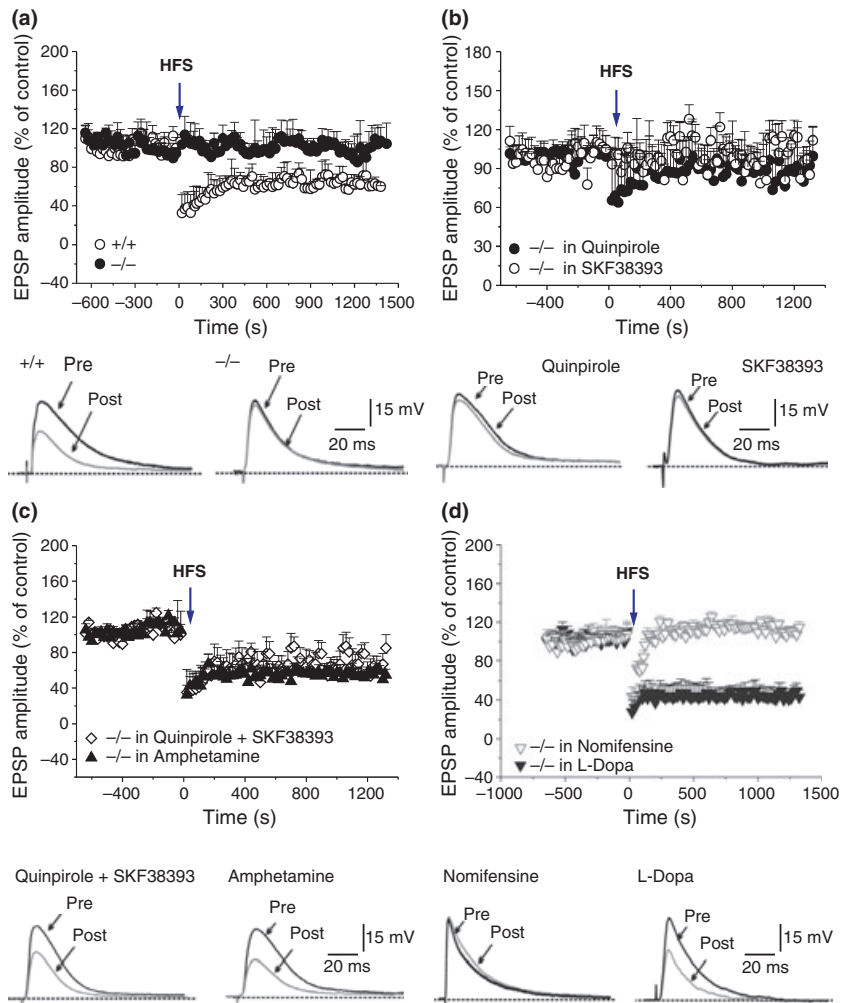


Fig. 3 Impaired corticostriatal LTD in *parkin* knockout mice. (a) HFS of corticostriatal fibers induced LTD of EPSP in striatal MSNs recorded from *parkin*^{+/+} mice (open circles), but failed to cause changes in synaptic efficacy in *parkin*^{-/-} mice (filled circles). The superimposed traces represent single EPSPs recorded before (pre) and 20 min after HFS (post) in *parkin*^{+/+}, and *parkin*^{-/-} mice, respectively. (b) Pre-treatment with the D₁-like receptor agonist SKF38393 (10 μ M) did not restore LTD (open circles). Likewise, incubation with the D₂-like agonist quinpirole (10 μ M) was unable to rescue LTD (filled circles). Representative traces are superimposed to show the EPSP recorded before (pre) and after (post, 20 min) HFS in slices from *parkin*^{-/-} mice. Data represent the mean \pm SEM of at least 8 independent

observations. (c) Time-course of EPSP amplitude after HFS in the presence of amphetamine (100 μ M, filled triangles) in the perfusing solution or after co-application of D₁ and D₂ receptor agonists, SKF38393 (10 μ M) plus quinpirole (10 μ M) (open diamonds). Under both these experimental conditions, LTD was restored in *parkin*^{-/-} mice. The traces superimposed show representative EPSPs recorded before (pre) and 20 min after HFS (post). Data are presented as mean \pm SEM of at least 6 experiments. (d) Pre-incubation with the DAT inhibitor nomifensine (100 μ M) did not rescue LTD (open triangles), whereas the DA precursor L-Dopa (100 μ M) restored LTD (filled triangles). Representative EPSPs recorded before and after HFS (pre and post, respectively). Each data point represents mean \pm SEM.

was able to induce LTD in the presence of both SKF38393 and quinpirole ($67.7 \pm 13\%$, $n = 7$, $p < 0.01$; Fig. 3c). The observation that the application of DA receptor agonists can restore LTD deficits implies that the impairment of corticostriatal LTD could not be attributed to intrinsic DA receptor dysfunction. Rather, it may result from a pre-synaptic DA release defect.

To test this notion, we pre-treated slices with amphetamine, which increased DA release, thereby increasing DA

availability in the synaptic cleft. Interestingly, pre-treatment with amphetamine (100 μ M, 20 min) fully restored LTD in MSNs of *parkin*^{-/-} mice ($63.1 \pm 15\%$, $n = 8$, $p < 0.01$; Fig. 3c). In a parallel set of experiments, slices were bathed with the DA precursor L-Dopa (100 μ M, 30 min). L-Dopa did not affect intrinsic and synaptic properties of the recorded neurons but fully restored LTD induction ($49.6 \pm 9.6\%$, $n = 6$, $p < 0.0001$; Fig. 3d). Additionally, to address the possible role of DAT in the lack of LTD, we bathed slices

with the selective DAT inhibitor, nomifensine (100 μ M, 20 min). However, nomifensine was unable to restore LTD in *parkin*^{-/-} mice ($110.3 \pm 5.8\%$, $n = 5$, $p > 0.05$; Fig. 3d).

Finally, in another set of experiments, we bathed the slices in a low magnesium-containing solution in order to optimize LTP induction (Calabresi *et al.* 1992). Under this experimental condition, HFS induced a robust LTP in *parkin*^{+/+} mice but failed to cause any change in synaptic efficacy in *parkin*^{-/-} mice (+/+ : $174.4 \pm 15.1\%$, $n = 8$, $p < 0.0001$; -/- : $96.3 \pm 9.3\%$, $n = 8$, $p > 0.05$; Fig. 4a). To test whether the defect in synaptic plasticity was specific to the glutamatergic synapse in the striatum, we explored the effects of *parkin* inactivation on NMDA receptor-mediated LTP in the Schaffer collateral pathway of the hippocampus in *parkin*^{-/-} mice, which was not modulated by the nigrostriatal dopaminergic input. *Parkin* inactivation did not affect LTP induced by five trains of TBS (Fig. 4b). The magnitude of LTP measured 60 min after induction ($150.6 \pm 6.9\%$) was unaffected in *parkin*^{-/-} mice relative to control mice ($154.0 \pm 7.0\%$, $p > 0.05$). This result showed that the synaptic plasticity was not altered in the Schaffer collateral pathway of the hippocampus in *parkin*^{-/-} mice.

Normal levels of DA receptors and DAT in the striatum

Our previous biochemical analysis measuring DA receptor levels using synaptic membrane fractions from the striatum showed unchanged levels of DA receptors in *parkin*^{-/-} mice (Goldberg *et al.* 2003). However, another analysis using autoradiography reported up-regulation of D₁ and D₂ receptors in *parkin*^{-/-} mice (Sato *et al.* 2006). Thus, we further examined whether loss of *parkin* altered the densities of striatal D₁ and D₂ receptors. Radioligand binding autoradiography had previously been used to demonstrate the abundance of D₁ and D₂ receptors in the striatum, as shown by high levels of binding to radioactively labeled antagonists of D₁- ([³H]-SCH23390) and D₂- ([³H]-spiperone) like receptors in the striatum (Kitada *et al.* 2007). We performed radioligand binding autoradiography to measure levels of surface D₁ and D₂ receptors in the striatum of *parkin*^{-/-} mice and wild-type controls using [³H]-SCH23390 and [³H]-spiperone (Fig. 5a). Quantitative analysis of binding densities in the striatum revealed no significant difference in the density of D₁ and D₂ receptors between the genotypic groups, suggesting normal levels of surface D₁ and D₂ receptors in the striatum of *parkin*^{-/-} mice (Fig. 5b). This result was consistent with our earlier study using a biochemical approach (Goldberg *et al.* 2003).

We also measured levels of DAT in the striatum of *parkin*^{-/-} mice using the [³H]DA reuptake assay (Copeland *et al.* 2005; Owens *et al.* 2005). [³H]DA uptake in *parkin*^{-/-} striatal membrane preparations (13.3 ± 1.4 pmol/mg, $n = 5$) was unchanged compared with wild-type controls (11.9 ± 2.3 pmol/mg, $n = 5$; Fig. 5c), consistent with the

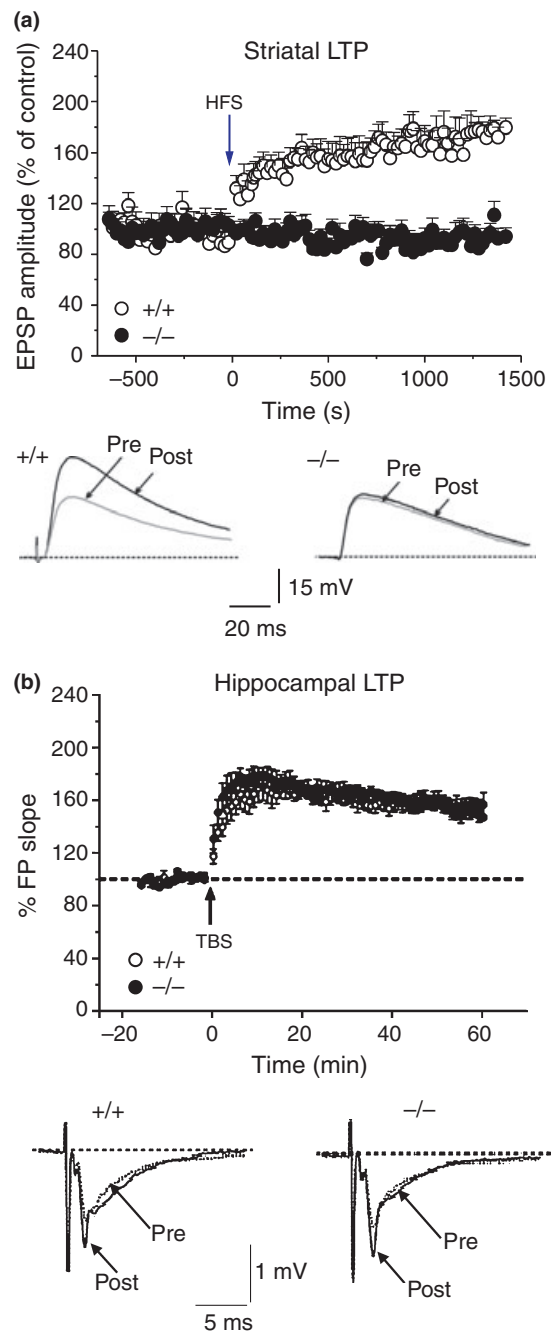


Fig. 4 Impaired corticostriatal LTP but normal hippocampal LTP in *parkin* knockout mice. (a) In the absence of external magnesium in the bathing solution, HFS induced a robust LTP in MSNs from *parkin*^{+/+} mice (open circles), whereas no change in synaptic efficacy was observed in *parkin*^{-/-} mice (filled circles). Superimposed EPSPs recorded before (pre) and 20 min after HFS (post) in *parkin*^{+/+}, and *parkin*^{-/-} mice, respectively. (b) Normal hippocampal LTP in *parkin*^{-/-} mice ($n = 6$ slices from three mice per genotype). LTP was induced by five episodes of TBS delivered at 0.1 Hz. Each episode contains ten stimulus trains (four pulses at 100 Hz) delivered at 5 Hz. Average responses (mean \pm SEM) are expressed as percent of pre-TBS baseline response.

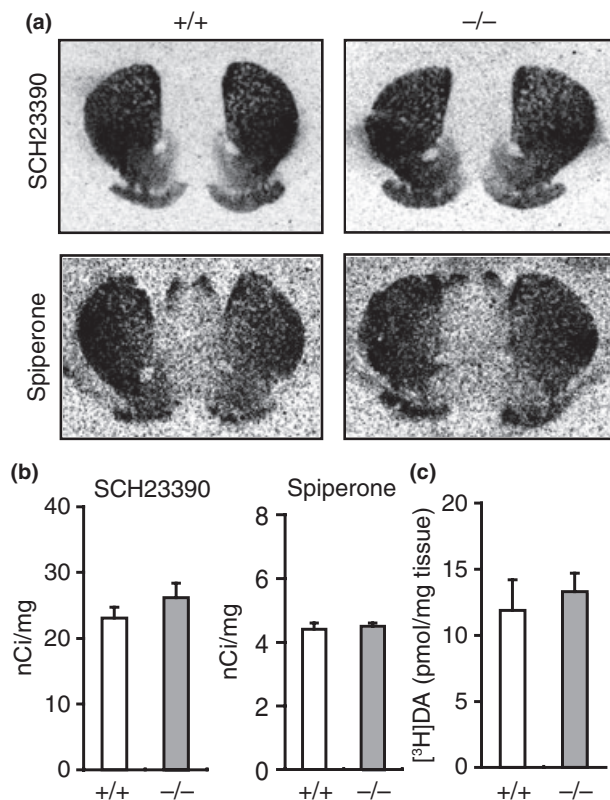


Fig. 5 Normal striatal levels of DA receptors and DAT in *parkin* knockout mice. (a) Representative images from ligand binding autoradiography show similar levels of binding of [³H]-SCH23390 and [³H]-spiperone to D₁ and D₂ receptors, respectively, in coronal sections through the striatum of *parkin*^{-/-} mice and wild-type controls. (b) Quantitative analysis of binding densities in the striatum revealed no significant difference in D₁ (SCH23390 in b) and D₂ receptors (Spiperone in b) between *parkin*^{-/-} mice and wild-type controls ($n = 4$ per genotype). (c) [³H]DA reuptake assay by DAT. [³H]DA uptake in *parkin*^{-/-} homogenate (13.3 ± 1.4 pmol/mg, $n = 5$) was unchanged compared with *parkin*^{+/+} homogenate (11.9 ± 2.3 pmol/mg, $n = 5$). Each data point represents the mean \pm SEM.

findings from amperometric recordings of striatal slices in the presence of nomifensine.

Discussion

Several reports of studies on the pathology in AR-JP brains concluded that loss of *parkin* causes a selective neuronal loss in substantia nigra pars compacta and locus coeruleus without any inclusion bodies or accumulation (Yamamura *et al.* 1993, 1996, 2000; Takahashi *et al.* 1994). This appears to be in conflict with the expected pathogenic mechanism by which *parkin* deficiency decreases proteolysis of target substrates. To gain insight into the pathogenic mechanism by which loss of *parkin* causes PD, we used a functional analysis approach to explore the normal function of Parkin in

dopaminergic synaptic transmission. Our results revealed an essential role for Parkin in the nigrostriatal circuit that was selectively affected in PD. The finding of decreased DA release from *parkin*^{-/-} slices was further supported by the results of decreased catecholamine release from dissociated adrenal chromaffin cells of *parkin*^{-/-} and *parkin*^{+/-} mice and impaired corticostriatal LTD and LTP in *parkin*^{-/-} slices. The deficits in striatal synaptic plasticity are likely to be a consequence of decreased DA release, as the LTD impairment can be rescued by L-Dopa and amphetamine, both of which increased DA release.

Parkin function in the dopaminergic circuit

Amperometric recordings in acute striatal slices demonstrated a significant reduction in electrically evoked DA signal in *parkin*^{-/-} mice. Evoked DA was affected by the balance between electrically stimulated DA release and DA reuptake by DAT. In the presence of nomifensine, which specifically blocks DA reuptake from DAT, evoked DA signals that were increased in both control and *parkin*^{-/-} slices, but the signal was still lower in *parkin*^{-/-} mice relative to the control, indicating that loss of Parkin indeed decreased DA release. Furthermore, using radioactively labeled DA we found similar amounts of radioactive DA taken by synaptosomes prepared from *parkin*^{-/-} and wild-type mice, suggesting normal DAT activity in the absence of parkin. Lastly, evoked catecholamine release from primary chromaffin cells which lacked the reuptake mechanism was also reduced in *parkin*^{-/-} mice, providing further support for a defect in exocytotic DA release. Interestingly, under basal conditions, extracellular DA levels measured *in vivo* using no net flux microdialysis were slightly increased in the striatum of *parkin*^{-/-} mice (Goldberg *et al.* 2003), suggesting that other processes contributing to basal DA levels, as measured by microdialysis, undergo compensatory changes. For instance, the mean interspike interval for catecholamine quantal events was smaller in *parkin*^{-/-} mice than in wild-type mice (data not shown). This meant that the frequency (i.e., number) of catecholamine quanta released upon stimulation was actually higher in the *parkin*^{-/-} group and could potentially overcome the decrease in the catecholamine quantal size, thereby resulting in similar or higher catecholamine levels in the extracellular space.

Dopamine release from nigral neurons to the striatum modulates excitatory corticostriatal synaptic transmission and plasticity. Our physiological analysis for the nigrostriatal circuit in *parkin*^{-/-} mice indicated a marked impairment in striatal synaptic plasticity. Inductions of LTD and LTP were impaired at in the striatal MSNs, the major target of nigrostriatal dopaminergic inputs. Consistent with the involvement of D₁ and D₂ receptors in LTD induction (Calabresi *et al.* 2007), impairment of LTD was rescued by agonists of both D₁ and D₂ receptors, which suggests normal receptor function. Administration of amphetamine, which

increased pre-synaptic DA release, and L-Dopa, which increased DA synthesis, also restored impaired LTD. However, nomifensine, which was shown to increase extracellular DA in both wild-type and *parkin*^{-/-} striatal slices by amperometry, failed to rescue LTD defect in *parkin*^{-/-} MSNs. This may be explained by the moderate increase in extracellular DA by nomifensine, whereas amphetamine and L-Dopa presumably increased evoked DA release in larger quantities and faster actions. Interestingly, LTP in the Schaeffer collateral pathway in hippocampus was unchanged compared with wild-type controls. These results suggest the deficits in striatal synaptic plasticity are caused by a specific defect in pre-synaptic dopaminergic function.

Implications for PD pathogenesis: reduced DA release as a common cellular precursor to neurodegeneration

Clinical features of PD are caused by reduced dopaminergic input to the striatum with progressive loss of nigral neurons. In addition to typical parkinsonian features, AR-JP patients exhibited specific symptoms such as sleep benefit/diurnal fluctuation. These symptoms implied hypersensitive and abnormal dopaminergic metabolism or signaling in these patients. This had been observed in patients carrying *DJ-1* and *PINK1* mutations as well (Bonifati *et al.* 2002; Dekker *et al.* 2003; Albanese *et al.* 2005). In search for a common, converging mechanism that underlies the pathogenesis of recessive parkinsonism, we conducted a series of genetic studies through the generation of mutant mice recapitulating genetic alterations in any of the three PD genes followed by multidisciplinary analysis. Our findings have demonstrated that these mouse models share a common cellular pathophysiological defect in the dopaminergic system. Specifically, evoked release of DA from nigral neurons was reduced in the absence of any of the three recessive PD genes (Goldberg *et al.* 2005; Kitada *et al.* 2007). However, as our study was limited to mice at one age, our study did not address age-related changes in the observed phenotypes.

Recent studies in *Drosophila* have also shown that *parkin* and *PINK1* null flies share similar phenotypes, such as indirect flight muscles and mitochondria (Clark *et al.* 2006; Park *et al.* 2006). Furthermore, the striking phenotypes exhibited by *PINK1*^{-/-} flies could be alleviated by over-expression of *parkin*, demonstrating that *PINK1* acts upstream of *Parkin* in a common pathway (Clark *et al.* 2006; Park *et al.* 2006). Although *parkin* and *PINK1* knockout mice did not exhibit such dramatic phenotypes, they did share similar mitochondrial respiration defects and DA release impairment with no effect on ATP and striatal DA content (Goldberg *et al.* 2003; Palacino *et al.* 2004; Kitada *et al.* 2007; Gautier *et al.* 2008). Recent reports on the effect of rotenone, a specific mitochondrial complex I inhibitor, showed that low doses of rotenone impaired DA release without affecting total DA content (Bao *et al.* 2005) and that striatal spiny neurons were much more sensitive than

hippocampal neurons to rotenone treatment (Costa *et al.* 2008). These new findings suggest that DA release is sensitive to inhibition of mitochondrial function, and that striatal spiny neurons are more sensitive to inhibition of mitochondrial than hippocampal neurons function. Therefore, although our studies have not addressed which of the two phenotypes, dopaminergic defects and mitochondrial dysfunction, may lead to or contribute to the development of the other phenotype, these *in vitro* studies provide evidence suggesting that mitochondrial dysfunction may contribute to the evoked DA release impairment.

Our series of genetic studies, along with these mitochondrial toxin studies, provide additional experimental evidence for dopaminergic defects and mitochondrial dysfunction being the proximal cause in the pathogenesis of PD (Shen and Cookson 2004). Elucidation of how loss of function mutations in these PD genes impair evoked DA release and induce nigral neurodegeneration will provide crucial information to better understand PD pathogenesis, which will permit better design of more effective therapeutic strategies.

Acknowledgements

We thank Douglas R. Porter and Huailong Zhao for assistance. This work was supported by grants from NINDS (ENP, JS), Michael J. Fox Foundation (JS), The Parkinson's Disease Foundation (ENP), Ministero Salute (Progetto Finalizzato) (AP), and Agenzia Spaziale Italiana (DCMC grant) (AP). The authors declare that they have no competing interests.

References

- Albanese A., Valente E. M., Romito L. M., Bellacchio E., Elia A. E. and Dallapiccola B. (2005) The *PINK1* phenotype can be indistinguishable from idiopathic Parkinson disease. *Neurology* **64**, 1958–1960.
- Bao L., Avshalomov M. V. and Rice M. E. (2005) Partial mitochondrial inhibition causes striatal dopamine release suppression and medium spiny neuron depolarization via H₂O₂ elevation, not ATP depletion. *J. Neurosci.* **25**, 10029–10040.
- Bonifati V., Breedveld G. J., Squitieri F. *et al.* (2002) Localization of autosomal recessive early-onset parkinsonism to chromosome 1p36 (*PARK7*) in an independent dataset. *Ann. Neurol.* **51**, 253–256.
- Calabresi P., Pisani A., Mercuri N. B. and Bernardi G. (1992) Long-term potentiation in the striatum is unmasked by removing the voltage-dependent Magnesium block of NMDA receptor channels. *Eur. J. Neurosci.* **4**, 929–935.
- Calabresi P., Picconi B., Tozzi A. and Di Filippo M. (2007) Dopamine-mediated regulation of corticostriatal synaptic plasticity. *Trends Neurosci.* **30**, 211–219.
- Ciolkowski E., Maness K., Cahill P., Wightman R., Evans D., Fosset B. and Amatore C. (1994) Disproportionation during electrooxidation of catecholamines at carbon-fiber microelectrodes. *Anal. Chem.* **66**, 36.
- Clark I. E., Dodson M. W., Jiang C., Cao J. H., Huh J. R., Seol J. H., Yoo S. J., Hay B. A. and Guo M. (2006) *Drosophila pink1* is required

- for mitochondrial function and interacts genetically with parkin. *Nature* **441**, 1162–1166.
- Copeland B. J., Neff N. H. and Hadjiconstantinou M. (2005) Enhanced dopamine uptake in the striatum following repeated restraint stress. *Synapse* **57**, 167–174.
- Costa C., Belcastro V., Tozzi A. *et al.* (2008) Electrophysiology and pharmacology of striatal neuronal dysfunction induced by mitochondrial complex I inhibition. *J. Neurosci.* **28**, 8040–8052.
- Dekker M., Bonifati V., van Swieten J. *et al.* (2003) Clinical features and neuroimaging of PARK7-linked parkinsonism. *Mov. Disord.* **18**, 751–757.
- Foroud T., Uniacke S. K., Liu L. *et al.* (2003) Heterozygosity for a mutation in the parkin gene leads to later onset Parkinson disease. *Neurology* **60**, 796–801.
- Gautier C., Kitada T. and Shen J. (2008) Loss of PINK1 causes mitochondrial functional defects and increased sensitivity to oxidative stress. *Proc. Natl Acad. Sci. USA* **105**, 11364–11369.
- Goldberg M. S., Fleming S. M., Palacino J. J. *et al.* (2003) Parkin-deficient mice exhibit nigrostriatal deficits but not loss of dopaminergic neurons. *J. Biol. Chem.* **278**, 43628–43635.
- Goldberg M. S., Pisani A., Haburcak M. *et al.* (2005) Nigrostriatal dopaminergic deficits and hypokinesia caused by inactivation of the familial Parkinsonism-linked gene DJ-1. *Neuron* **45**, 489–496.
- Hattori N., Kitada T., Matsumine H. *et al.* (1998) Molecular genetic analysis of a novel Parkin gene in Japanese families with autosomal recessive juvenile parkinsonism: evidence for variable homozygous deletions in the Parkin gene in affected individuals. *Ann. Neurol.* **44**, 935–941.
- Hedrich K., Eskelson C., Wilmot B. *et al.* (2004) Distribution, type, and origin of Parkin mutations: review and case studies. *Mov. Disord.* **19**, 1146–1157.
- Kitada T., Asakawa S., Hattori N., Matsumine H., Yamamura Y., Minoshima S., Yokochi M., Mizuno Y. and Shimizu N. (1998) Mutations in the parkin gene cause autosomal recessive juvenile parkinsonism. *Nature* **392**, 605–608.
- Kitada T., Pisani A., Porter D. R. *et al.* (2007) Impaired dopamine release and synaptic plasticity in the striatum of PINK1-deficient mice. *Proc. Natl Acad. Sci. USA* **104**, 11441–11446.
- Lucking C. B., Durr A., Bonifati V. *et al.* (2000) Association between early-onset Parkinson's disease and mutations in the parkin gene. *N. Engl. J. Med.* **342**, 1560–1567.
- Martella G., Platania P., Vita D. *et al.* (2009) Enhanced sensitivity to group II mGlu receptor activation at corticostriatal synapses in mice lacking the familial parkinsonism-linked genes PINK1 or Parkin. *Exp. Neurol.* **215**, 388–396.
- Owens W. A., Sevak R. J., Galici R., Chang X., Javors M. A., Galli A., France C. P. and Daws L. C. (2005) Deficits in dopamine clearance and locomotion in hypoinsulinemic rats unmask novel modulation of dopamine transporters by amphetamine. *J. Neurochem.* **94**, 1402–1410.
- Palacino J. J., Sagi D., Goldberg M. S., Krauss S., Motz C., Wacker M., Klose J. and Shen J. (2004) Mitochondrial dysfunction and oxidative damage in parkin-deficient mice. *J. Biol. Chem.* **279**, 18614–18622.
- Park J., Lee S. B., Lee S. *et al.* (2006) Mitochondrial dysfunction in *Drosophila* PINK1 mutants is complemented by parkin. *Nature* **441**, 1157–1161.
- Sato S., Chiba T., Nishiyama S. *et al.* (2006) Decline of striatal dopamine release in parkin-deficient mice shown by ex vivo autoradiography. *J. Neurosci. Res.* **84**, 1350–1357.
- Saura C. A., Choi S. Y., Beglopoulos V. *et al.* (2004) Loss of presenilin function causes impairments of memory and synaptic plasticity followed by age-dependent neurodegeneration. *Neuron* **42**, 23–36.
- Shen J. and Cookson M. R. (2004) Mitochondria and dopamine: new insights into recessive parkinsonism. *Neuron* **43**, 301–304.
- Shimura H., Hattori N., Kubo S. *et al.* (2000) Familial Parkinson disease gene product, parkin, is a ubiquitin-protein ligase. *Nat. Genet.* **25**, 302–305.
- Sun M., Latourelle J. C., Wooten G. F. *et al.* (2006) Influence of heterozygosity for parkin mutation on onset age in familial Parkinson disease: the GenePD study. *Arch. Neurol.* **63**, 826–832.
- Takahashi H., Ohama E., Suzuki S., Horikawa Y., Ishikawa A., Morita T., Tsuji S. and Ikuta F. (1994) Familial juvenile parkinsonism: clinical and pathologic study in a family. *Neurology* **44**, 437–441.
- Yamamura Y., Sobue I., Ando K., Iida M. and Yanagi T. (1973) Paralysis agitans of early onset with marked diurnal fluctuation of symptoms. *Neurology* **23**, 239–244.
- Yamamura Y., Arihiro K., Kohriyama T. and Nakamura S. (1993) Early-onset parkinsonism with diurnal fluctuation: clinical and pathological studies. *Rinsho Shinkeigaku* **33**, 491–496.
- Yamamura Y., Kohriyama T., Kawakami H., Kaseda Y., Kuzuhara S. and Nakamura S. (1996) Autosomal recessive early-onset parkinsonism with diurnal fluctuation (AR-EPDF)—clinical characteristics. *Rinsho Shinkeigaku* **36**, 944–950.
- Yamamura Y., Hattori N., Matsumine H., Kuzuhara S. and Mizuno Y. (2000) Autosomal recessive early-onset parkinsonism with diurnal fluctuation: clinicopathologic characteristics and molecular genetic identification. *Brain Dev.* **22**(Suppl 1), S87–S91.